





Diagnostic Analysis on Change Vector Analysis Methods for LCCD Using Remote Sensing Images

Lv ZhiYong , *Member, IEEE*, FengJun Wang, LinFu Xie, WeiWei Sun , *Senior Member, IEEE*, Nicola Falco , *Member, IEEE*, Jón Atli Benediktsson , *Fellow, IEEE*, and ZhenZhen You

Abstract—Change vector analysis (CVA) is a simple yet attractive method to detect changes with remote sensing images. Since its first introduction in 1980, CVA has received increased attention from the remote sensing community, leading to the definition of several new methodologies based on the CVAs concept while extending its applicability. In this article, we provide an extensive review of CVA-based approaches in the context of land-cover change detection (LCCD). We first reviewed the development of the CVA-based LCCD method with remote sensing images, and some classical-related methods were discussed. Then, we analyze and compare the performance of five selected methods. The analysis was carried out on seven real datasets acquired by different sensors and platforms (e.g., Landsat, Quick Bird, and airborne) and spatial resolutions (from 0.5 to 30 m/pixel), with scenes from both urban and natural landscapes. The analysis shows several findings, which include that the performance of CVA-based approaches is, in general, resolution dependent, and the detection accuracies of a specific method vary with different input datasets, for example, when applying the classical CVA to the datasets with a resolution from 0.5 to 30 m/pixel, the accuracy of false alarm (FA) ranges from 2.26% to 23.22%. Furthermore, the diagnoses also remind that the detection accuracies for a specific method varied with the size of the area being considered for a given dataset, such as when applying deep CVA (DCVA) to the image with 200×200 to 1600×1600 size of the Landsat dataset, the FA of DCVA reduced from 11.8% to 1.0%. Moreover, comparing the detection accuracies of different methods implies that the content of an image scene still plays an important role when disregarding the unique preferences of different methods.

Index Terms—Change vector analysis (CVA), land-cover change detection (LCCD), remote sensing images.

I. INTRODUCTION

THE continuous development and improvement of remote sensing technology for Earth observation has enabled new capabilities in characterizing and monitoring natural phenomena and human activities from local to global scale. The ability to acquire multitemporal and time-series remote sensing images allows us to capture and model spatial–temporal dynamics covering the Earth’s surface. These remote sensing images used for observing the Earth’s surface usually referred as hyperspectral images [2], [3], very high resolution images [4], and low-median resolution images [5].

Change detection analysis is a particular procedure that aims to identify occurred changes within an area under investigation. This procedure requires algorithms able to analyze multitemporal acquisitions and extract meaningful information related to the occurred changes. Change detection analysis is one of the main research subjects in remote sensing and represents an important task in practical applications [4], [6]. One of these application is the detection of changes in land covers [land-cover change detection (LCCD)], such as changes due to landslides [7], [8], changes in urban areas and building structure [9]–[11], and environmental protection [12]. Several change detection approaches have been proposed in the literature but change vector analysis (CVA) [13] represents one of the most widely used techniques to solve the change detection task across scenarios and datasets. Because of its simple mathematical definition, several methodologies have been developed around the CVA concept. In this article, we provide an overview of the CVA-based methods that are currently available in the literature and used for LCCD applications. Then, we give a comprehensive diagnosis on the performance of six selected methods with different datasets. These methods include the classical CVA [13], the CVA coupled with Markov random field (CVA_MRF) [14], the CVA integrated with the spectral angle mapper (CVA_SAM) [15], robust CVA (RCVA) [16], deep CVA (DCVA) [1], and tritemporal logic-verified CVA (TLCVA) [17], which are widely used for LCCD with remote sensing images. More details about these methods will be presented in the following sections.

II. OVERVIEW OF CVA-BASED METHODS

The classical CVA was first briefly defined by Malila in [13] and applied it to detect forest changes with Landsat images. Due

Manuscript received July 29, 2021; revised September 7, 2021; accepted September 22, 2021. Date of publication September 27, 2021; date of current version October 18, 2021. This work was supported in part by the National Natural Science Foundation of China under Grants 61701396, 42001407, and 41971296, in part by the Guangdong Basic and Applied Basic Research Foundation under Grant 2019A1515110729, and in part by the Open Fund of Key Laboratory of Urban Land Resources Monitoring and Simulation, MNR under Grant KF-2019-04-042. (Corresponding author: LinFu Xie.)

Lv ZhiYong, FengJun Wang, and ZhenZhen You are with the School of Computer Science and Engineering, Xi’an University of Technology, Xi’an 710048, China (e-mail: Lvzhijong@hotmail.com; Wangfengjun_Run@hotmail.com; zhenzhen_you@xaut.edu.cn).

LinFu Xie is with the Guangdong Key Laboratory of Urban Informatics and Key Laboratory of Urban Land Resources Monitoring and Simulation, MNR and Research Institute for Smart Cities, School of Architecture and Urban Planning, Shenzhen University, Shenzhen 518060, China (e-mail: linfuxie@szu.edu.cn).

WeiWei Sun is with the Department of Geography and Spatial Information Techniques, Ningbo University, Ningbo 315211, China (e-mail: nb-sww@outlook.com).

Nicola Falco is with Lawrence Berkeley National Laboratory in the Climate and Ecosystem Sciences Division (CESD), Berkeley, CA 94720 USA (e-mail: nicolafalco@lbl.gov).

Jón Atli Benediktsson is with the Faculty of Electrical and Computer Engineering, University of Iceland, IS-107 Reykjavik, Iceland (e-mail: benedikt@hi.is).

Digital Object Identifier 10.1109/JSTARS.2021.3115481

TABLE I
BRIEF SUMMARY OF CVA-BASED LCCD APPROACHES WITH REMOTE SENSING IMAGES

Concentration	Characteristics	Referred Literature
Application	Studies that use the classic CVA to solve the change detection task in specific scenarios	<ol style="list-style-type: none"> 1.Forest changes [13], [36]–[41]; 2.Vegetation change [42]–[48]; 3.land cover change of drought indices [47]–[49]; 4.Change detection of ecosystem [50]–[54]; 5.Land cover change motioning in forest and ecosystem [38], [51], [55]–[58]; 6.Referreed water change [59], [60]; 7.Urban growing motoring [61]; 8.Fire risk assessment [62]; 9.Apply CVA on multi-features [63]; 10.Apply CVA on Hyperspectral images [26], [64], [65]; 11.Apply CVA on SAR images [66], [67] and Lidar [68];
Algorithm	Studies that integrate or extend the standard CVA to improve the detection performance	<ol style="list-style-type: none"> 1.CVA-based tool [18], [69]; 2.Extended CVA to multi-temporal space [24], [43], [61], [70]–[72]; 3.Cosine CVA [73]; 4.Median CVA [74]; 5.CVA in polar domain [39], [75], [76]; 6.Fusion based on pixel-level CVA and multivariate regression [77]; 7.Land cover change category [38], [78]–[80]; 8.Object-level CVA [25], [29]–[32]; 9.CVA based on distance and similarity measures [81]; 10.CVA in posterior probability space [82]–[84]; 11.Adaptive CVA [33], [34]; 12.CVA and deep learning techniques [1], [17], [85], [86]; 13.Robust CVA [16]; 14.Spectral angle mapper and CVA [15], [64]; 15.Compressed CVA [35], [87]; 16.Fuzzy CVA [88]; 17.Multivariate CVA [40];

to the better performance and easily to be applied in practice, CVA has been widely used in detecting land cover change with remote sensing images in many aspects. Lambin *et al.* applied CVA in a multitemporal space with local area coverage imagery obtained by the NOAA-9 and NOAA-11 orbiting platforms. That study clearly reveals the nature and magnitude of the land cover change in the region of West Africa [18]. Consequently, Labmin *et al.* [19] also applied CVA to three remote sensing indicators (vegetation index, surface temperature, and spatial structure) to capture and categorize subtle forms of land cover changes with the NOAA-9 and NOAA-11 datasets. As well as Bayarjargal *et al.* [20] built three drought indices (normalized difference vegetation index, standardized vegetation index, and vegetation condition index) to compare the spatial occurrences of droughts using CVA with NOAA images.

Allen *et al.* [21] applied spherical statistics to CVA to detect the change of fir forests in Southern Appalachian, this study demonstrated the ability of CVA in multiple biophysical dimensions to differentiate forest disturbance and regeneration trends. Siwe *et al.* used CVA to categories land cover change with bitemporal series of Landsat images. Here, in order to present an overview of the various application of CVA-based change detection, a brief summary is presented in Table I. From these applications, it can be found that, like any other change detection techniques, CVA-based LCCD approaches also requires two primiparity dataset processing, image to image geometric registration and radiometric normalization [22]. Moreover, CVA is widely applied, but one of its intractable tasks is the determination of a binary threshold to acquire the detection map [23].

Apart from the application extensions of CVA methods, CVA-based LCCD algorithms have also been extended in many ways from the viewpoint of methodology. For example, the classical CVA has been extended to multitemporal spaces in order to deal with the challenge of standard CVA on calculating change magnitude (CM) and direction in a high-dimensional feature space [24] and multidimensional CVA has been developed successfully for LCCD with remote sensing images [25]. One obvious difference between these extended CVA approaches and the classical CVA lies in the processing ability of feature bands. To apply CVA on hyperspectral images, Liu *et al.* defined a sequential spectral CVA (S^2CVA), which is based on a compressed change representation in a 2-D polar domain and defined by two change variables (magnitude and direction) for detecting change in hyperspectral images [26], [27], the advantage of S^2CVA lies in that it can be applied in hyperspectral images and to detect a large number of major and subtle changes. Instead of using spectral bands directly as in the classical CVA, Junior *et al.* [28] suggested to estimate the CM by a distance measurement and measure the change direction by a similarity approach based on the spectral angle mapper (SAM) and spectral correction similarity, respectively. The main advantage of the approach in [28] lies in that it generates a single image of change information insensitive to illumination variation. Another related approach to the one proposed in [28] is by Zhuang *et al.* [15] who promoted two strategies, called hybrid feature vector and autoadapted fusion strategy, to combine SAM and CVA at the original feature level to improve detection accuracies. In addition, the processing unit of CVA has been extended from pixel to object for further smoothening salt-and-pepper noise in the detection map while using remote sensing images with a very high spatial resolution [29]–[31]. Self-adaptive weight CVA has also been adopted in some studies to cover the various shapes of ground targets [32], [33]. Overall, the classical CVA has been extended in many ways for LCCD with remote sensing images, such as robust CVA (RCVA) [16], which developed to account for pixel neighborhood effects, multiscale CVA [34], and an improved CVA named TLCVA [17] that can identify the errors of CVA through logical reasoning and judgment with an additional temporal image assistance. Recently, deep learning has been integrated with CVA for LCCD with remote sensing images, such as a context-sensitive framework called DCVA was developed for exploiting convolutional neural network features [1]. Markov random field was suggested to couple with CVA (MRF_CVA) to utilize the contextual information and acquire a better detection performance [14]. To present an overview of the extension of the classical CVA and the referred practical applications, we summarized the various studies in Table I according to the various applications in which CVA was used as well as its further extension/integration within new methodologies.

The summary in Table I indicates that CVA has been successfully applied in different scenarios and for different targets. At the same time, there is an active on-going research in defining new methods that extend or integrated the CVA concept. Several studies [5], [83]–[86] can be found that focus on reviewing LCCD techniques, indicating the development of CVA-based change detection techniques as an important branch of LCCD with remote sensing images. However, there are no studies that

focus on the CVA-based methods specifically. To the best of our knowledge, this would be the first study focused on CVA and its various developments.

In this article, we first review and summarize the characteristics of CVA-based LCCD methods. Then, we implement some selected and widely used CVA-based LCCD methods on six different datasets to investigate the performance and adaptability of each technique on different datasets. This article aims to investigate some typical CVA-based change detection techniques quantitatively and test the adaptability of the CVA-based approach for different images. This objective and quantitative investigation of these typical methods may be helpful for promoting the development of CVA-based LCCD methods and extending their applications.

III. CVA-BASED CHANGE DETECTION

According to the concept of classical CVA mentioned in [13], for the bitemporal pairs of spectral measurements, CVA-based methods usually provide two outputs: magnitude and phase. The magnitude provides a measure of how much it changed, a binary map can be obtained by applying a threshold, several methods can be used to perform the thresholding [66], [87]. In addition, someone can actually perform ROC curves to identify the best point that minimize false/predicted alarms [88]. In addition, the phase refers to the angle of change, the angle between the vector and horizontal level is defined as the direction to illustrate the different types of change. The calculation of the CM and the phase or change direction (θ) is presented as follows:

$$\text{CM} = \sqrt{\sum_{i=1, j=1}^{i=N, j=B} (D_{i,j}^{c,r} - D_{j,i}^{c,r})^2} \quad (1)$$

$$\theta = \arccos \left[\frac{1}{\sqrt{B}} \left(\sum_{i=1, j=1}^{i=N, j=B} D_{i,j}^{c,r} \right) \right. \\ \left. / \left(\sqrt{\sum_{i=1, j=1}^{i=N, j=B} (D_{i,j}^{c,r} - D_{j,i}^{c,r})^2} \right) \right] \quad (2)$$

where CM is the change magnitude between the multitemporal images. N and B denote the total number of images and spectral bands, respectively. D_{ij} is the pixel values in band j for date i at a position (c, r) located by c -column and r -row. From the aforementioned discussion, it can be seen that the realization of the CVA-based approach relies on entirely contiguous pixels and the spectral bands of the bitemporal images. The size of change vector between the bitemporal images indicates CM image. Moreover, due to the different ground targets have different spectral reflectance at each band, CVA can obtain the change information among different classes by analyzing the CM of angle. Therefore, the advantage of CVA lies in avoiding the loss of spectral information for each band.

The characteristics of the CVA-based LCCD approach can be briefly summarized as follows:

- 1) detecting change based on CVA can be defined as a radiometric technique, and these methods based on CVA can quantify the CM and illustrate the change types [18], [22];

- 2) CVA-based LCCD method can deal with bitemporal images with the same number of spectral bands [57], [83];
- 3) as well as other LCCD methods, CVA-based LCCD method can capture the change information over multiple intervals through observing the spatial-temporal trajectory with multitemporal images [22].

However, CVA-based LCCD methods also have several drawbacks that limit their practical application.

- 1) Due to CVA-based LCCD methods is a digital processing technique that measure the spectral radiometric change, the calculation of CVA-based LCCD methods require accurate coregistration and spectral co-correction for measuring CM between bitemporal or multitemporal images [66].
- 2) An image scene usually covers different ground objects; different image scene will generate different change magnitude image. Thus, it is difficult to cover all kinds of change types using one single threshold [35], [89].

In the following section, we selected six typical and widely used methods, including the classical CVA [13], CVA_MRF [14], CVA_SAM [15], RCVA [16], DCVA [1], and TLCVA [17], for comprehensive diagnosis and analysis. Details of the analysis are presented in the experimental section.

IV. MATERIALS AND METHODS

In this section, to present a comprehensive diagnosis on the CVA-based LCCD methods, we designed two experiments to achieve the following objectives.

- 1) To investigate the performance and adaptability of the six selected CVA-based LCCD methods, we design the first experiment based on six datasets acquired by different platforms at different resolutions.
- 2) The second experiment aims to test the relationship between the detection accuracies and input image size for a given dataset and a specific method.

Notably, the effect from the following aspects in the two experiments is neglected.

- 1) The various influences of the different scenes on the detection accuracies of a given algorithm is neglected.
- 2) The different separability degrees between the background and detecting targets of different datasets are ignored for a specific algorithm.
- 3) Different imaging conditions may affect the observations for different platforms and sensors, and this affection is neglected in the following experiments.

On the basis of the two preassumptions, the adaptability of the algorithm is investigated with the datasets of different resolutions and land cover change types. The relationship between image size and detection accuracies for an algorithm is achieved by increasing the size of an image scene. Details of the experiments are presented in the following subsections.

A. Remote Sensing Datasets

For the first experiment, we selected six datasets [dataset-a, ..., dataset-f, shown in Fig. 1(a)–(f)] acquired from different sensors including Landsat, Quick Bird, and airborne, and

covering spatial resolution from 0.5 to 30 m/pixel. Moreover, different change types are considered for the analysis, including changes in vegetation, urban areas, land-use, and natural phenomena such as landslides.

In the second experiment, apart from the dataset-c, another dataset acquired by Landsat-5 satellite (shown in Fig. 2) is adopted for investigating the relationship between image size and detection accuracies. The images were acquired in July 2000 and July 2006, have a spatial resolution of 30-m/pixel resolution. The scene depicts forest deformations in the Amazon forest in Rondônia, Brazil. The size of this study area is 2000×2000 pixels. The two datasets adopted in the second experiment are resized into different image scenes, as shown in Fig. 3. The upper left corner of each resized image block is fixed, and the length and width of each resized image block are gradually increased by 200 pixels for resizing the image into different image blocks.

B. CVA-Based Techniques

In the experiments, we choose six widely used unsupervised LCCD methods to achieve the testing aims without the effect from parameter setting. These methods are the most widely used typical CVA [8], the CVA coupled with Markov random field (CVA_MRF) [14], CVA integrated with spectral angle mapper (CVA_SAM) [15], robust CVA (RCVA) [16], deep CVA (DCVA) [1], and TLCVA [17]. When the CM images based on the selected methods are obtained, the widely used binary threshold method called Otsu [87] is used to obtain the binary change detection map. In addition, three widely used evaluation measurements are utilized for evaluation to quantitatively analyze the detection accuracies of the selected methods [90]. The measurements are false alarm (FA), missed alarm (MA), and total error (TE). Here, some abbreviations are defined as follows for clearly demonstrating the meaning of the three measurements: UC is the number of changed pixels in the detection map that is unchanged in the ground reference, CU is the number of unchanged pixels in the detection map that is changed in the ground reference, TRC is the total number of changed pixels in the ground reference, and TRU is the number of unchanged pixels in the ground reference. Based on these assumptions, these measurements can be defined as $FA = \frac{UC}{TRU} \times 100\%$, $MA = \frac{CU}{TRC} \times 100\%$, and $TE = \frac{UC+CU}{TRU+TRC} \times 100\%$, respectively. The details of each experiment based on these measurements are presented in the next section.

C. Results and Discussion

The results of the first experiments are presented in Tables II–IV in terms of FA, MA, and TE, respectively. As shown in Table II, the selected approaches are applied to Landsat images with a 30-m/pixel resolution, and their detection accuracies are better than 5.0% in terms of FA. However, the FA of each approach does not improve with the increase in image resolution, as shown in Fig. 4. In addition, CVA_MRF [14], CVA_SAM [15], and TLCVA [17] exhibit a horizontal trend with the increase in resolution. All the methods show similar detection accuracies for the FA measurement on a specific dataset. For example, in terms of FA for the Data-f, their accuracies range from 14.91% to

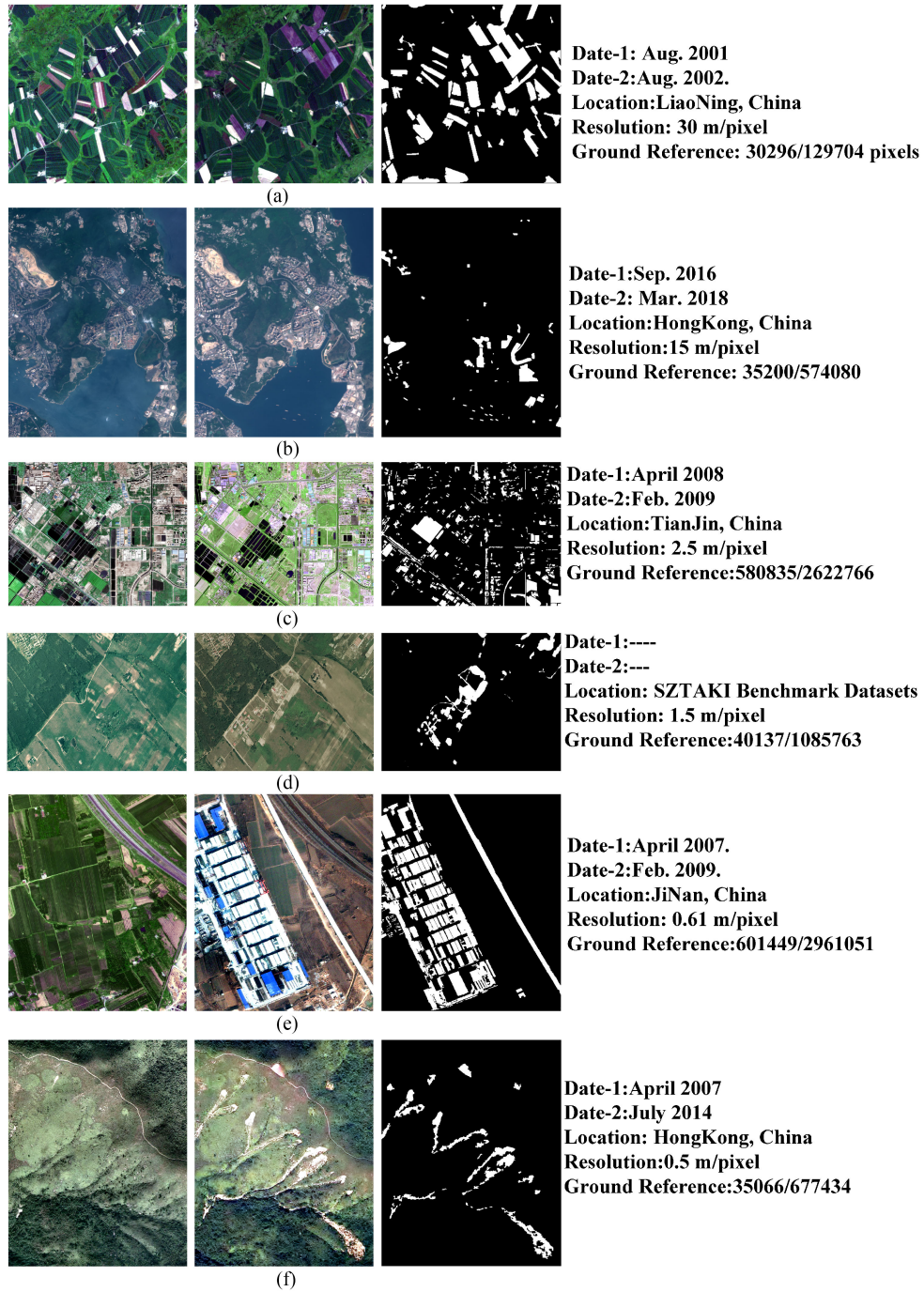


Fig. 1. Dataset and corresponding details for each of the areas and their reference maps (Ground reference denoted $\frac{a}{b}$, a is the number of changed pixels and b is the number of unchanged pixels).

TABLE II
COMPARISONS AMONG DIFFERENT METHODS IN TERMS OF FA (%)

Dataset	Resolution	CVA [13]	CVA_MRF [14]	CVA_SAM [15]	RCVA [16]	DCVA [1]	TLCVA [17]
1	30 m/pixel	4.53	4.65	3.71	0.81	1.78	1.51
2	15 m/pixel	19.33	10.92	9.8	1.91	11.88	18.74
3	2.5 m/pixel	23.22	20.22	22.69	17.3	0.87	17.2
4	1.5 m/pixel	2.26	22.74	21.58	10.97	7.64	19.11
5	0.61 m/pixel	15.01	18.74	19.64	19.44	19.28	14.91
6	0.5 m/pixel	15.06	19.6	14.91	7.55	18.41	17.01

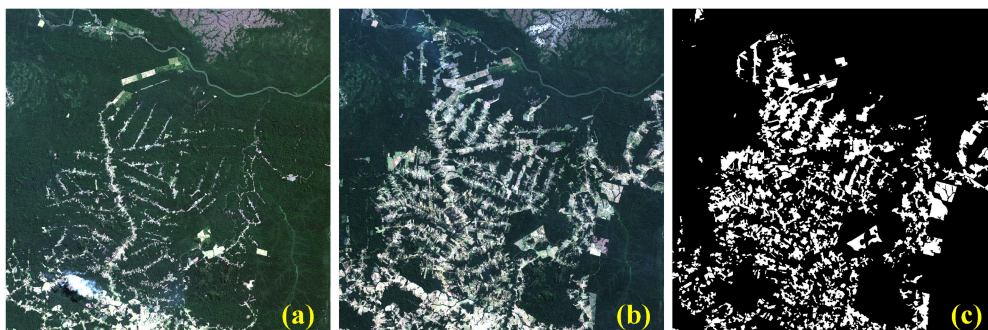


Fig. 2. Landsat images of forest deformation. (a)–(c) Preevent image, postevent image, and the ground reference map, respectively.

TABLE III
COMPARISONS AMONG DIFFERENT METHODS IN TERMS OF MA (%)

Dataset	Resolution	CVA [13]	CVA_MRF [14]	CVA_SAM [15]	RCVA [16]	DCVA [1]	TLCVA [17]
1	30 m/pixel	10.16	39.47	37.34	60.03	50.34	19.83
2	15 m/pixel	32.07	35.6	40.85	61.07	87.02	38.31
3	2.5 m/pixel	25.78	27.86	24.51	29.94	73.17	28.31
4	1.5 m/pixel	37.44	2.14	5.04	7.598	43.21	2.69
5	0.61 m/pixel	44.01	40.44	48.28	48.62	17.76	44.24
6	0.5 m/pixel	18.53	15.94	27.89	37.54	31.1	17.32

TABLE IV
COMPARISONS AMONG DIFFERENT METHODS IN TERMS OF TE (%)

Dataset	Resolution	CVA [13]	CVA_MRF [14]	CVA_SAM [15]	RCVA [16]	DCVA [1]	TLCVA [17]
1	30 m/pixel	5.59	11.24	10.07	12.02	10.97	4.981
2	15 m/pixel	19.97	11.8	10.91	4.01	14.56	19.44
3	2.5 m/pixel	21.81	19.58	21.24	17.42	8.67	17.34
4	1.5 m/pixel	9.21	18.67	18.31	10.31	14.67	15.87
5	0.61 m/pixel	16.68	19.99	21.29	21.13	19.2	44.24
6	0.5 m/pixel	15.23	19.42	15.55	9.03	18.78	17.02

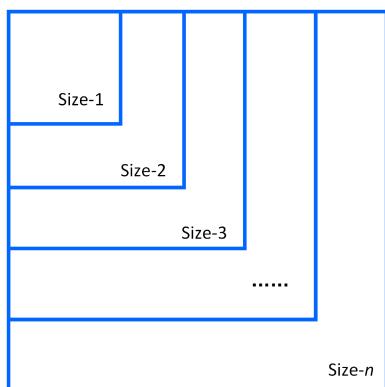


Fig. 3. Demonstration the strategy of image resizes for the second experiment.

19.64%. Observing the MA of each approach for each dataset in Table III clearly presents that each approach performs differently for the Landsat dataset with 30 m/pixel. When the resolution of the dataset is increased, the MA of each approach becomes better and exhibits a stable trend. The relationship between detection

accuracies and dataset resolution presents a similar characteristic in terms of TE for the selected approaches, as shown in the third row of Fig. 4.

The diagnosis on the results of the selected methods in the first experiment demonstrates the following observations.

- 1) High resolution does not mean high detection accuracies for the problem of LCCD with remote sensing images. The detection accuracies in terms of FA, MA, and TE will not increase with the increase in image resolution for a specific method. Although the increment in the spatial resolution of an image improves the visual performance and the details of ground objects can be captured and described clearly, the correlation among pixels is tighter than that of low-median resolution images and the mixed pixels are increased. Therefore, the spectral homogeneity of an object becomes low, the pixels constructing the object may be difficult to be detected, and the salt-and-pepper noise of the detection maps may be increased.
- 2) Although the detection accuracies of different methods may vary with the distinct datasets, most of the methods pose similar detection accuracies for a particular

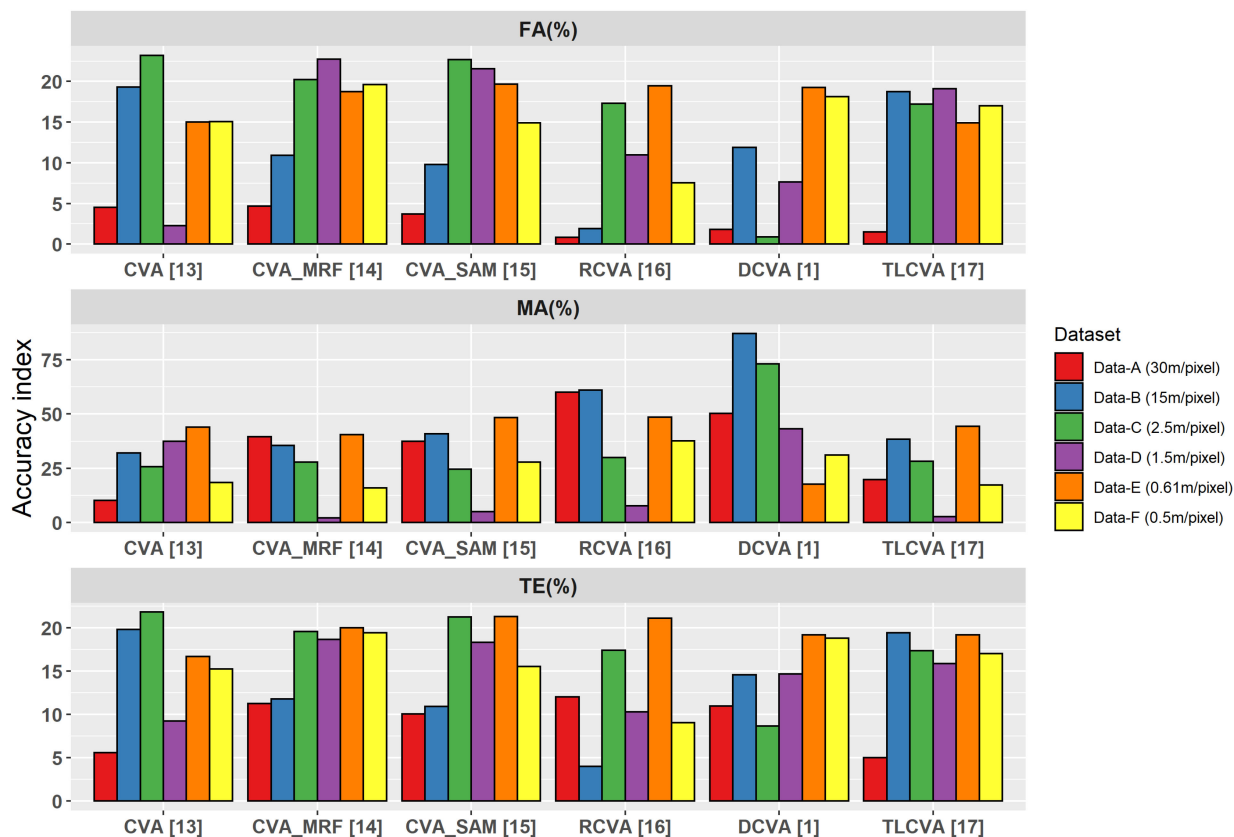


Fig. 4. Relationship among detection accuracies, datasets with different resolutions, and different methods in terms of FA, MA, and TE.

dataset, especially when the resolutions are 30, 0.61, and 0.5 m/pixel. This result may be due to that the nature of the data plays a decisive role in the progress of change detection even if some methods may have a bias preference for a specific dataset. The comprehensive diagnosis achieved by comparative bars, as shown in Fig. 4, further verifies the correctness of this perspective. The comparative bars imply that different methods perform similar detection accuracies for the same datasets, especially for FA on Data-a, as shown in Fig. 4. The relationship between the resolution and the detection accuracies in terms of MA and TE are shown in Fig. 4 for further observation.

To investigate the relationship between detection accuracies and input image size, the second experiment is performed on Landsat images with a 30-m/resolution and Spot-5 images with 2.5 m/pixels to achieve this objective. From the image scene in Fig. 2, it can be seen that the Landsat images depict forest deformation, trees, and the felling district. Thus, it assumed that the influences from the different content of different input image blocks are neglected in the comparisons and observation. Based on the fact of assumption, diagnosing the relationship between the size of the input image and detection accuracies for a specific method shows the following observations.

- 1) Different methods have a different response to the size of input images in terms of FA, MA, and TE. As shown in the first row of Fig. 6, the detection accuracies of DCVA [1] decrease with the increase in image size, and the

accuracies reach the best performance when the image size is 400×400 pixels. Then, when the image size is larger than 400×400 pixels, MA and TE increase, and then, exhibit a horizontal level. However, FA has no observational pattern. Comparing the curve of DCVA [1] with those of RCVA [16] and CVA_SAM [14] implies that the different curve shapes indicate their distinct responses to the same size of input image. The visual performance shown in Fig. 5 well supported this observation. For example, when observe the performance of the classical CVA [13] method at the first column, it can be seen that the noise performed on the result of Dataset-a is less than that of Dataset-f, that may be caused by the difference of spatial resolution; and when observe the performance at the first row, it can be found that different methods presented different performance on the same dataset, that is because the different detection ability of different methods.

- 2) The methods demonstrate different responses to the same sizes of input images for varying datasets. This is shown, e.g., in the first rows of Figs. 6 and 7, where DCVA [1] has different responses to the same size image scene from the Landsat and Spot images. A similar conclusion can be acquired while observing the response of RCVA [16] and CVA_SAM [15] methods in Figs. 6 and 7. The visual performance is presented in Figs. 8 and 9. From these observations, despite the visual performance for a specific method seems similar, while the size of the inputting

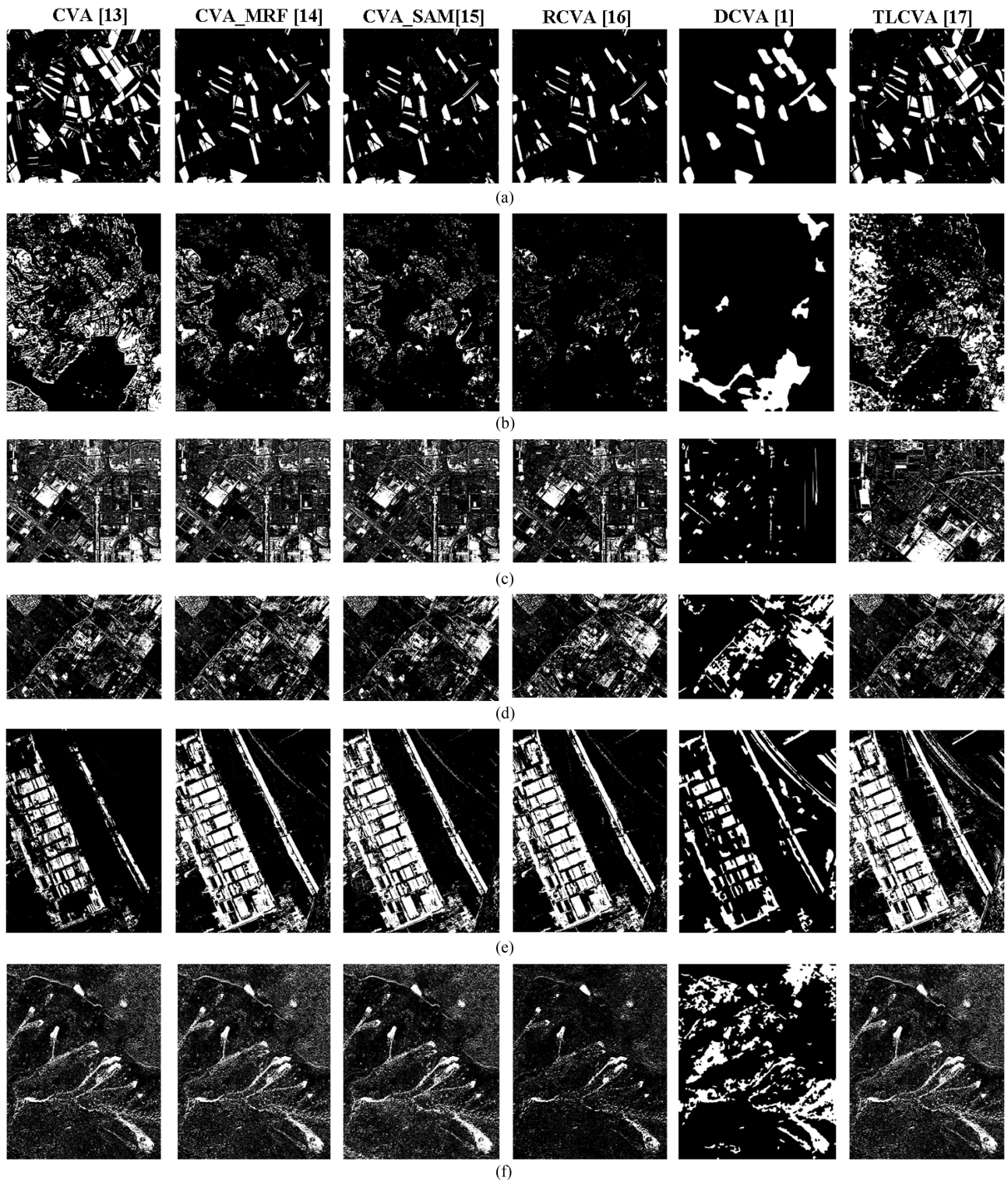


Fig. 5. Visual performance comparisons based on the six datasets with the selected approaches: CVA [13], CVA_MRF [14], CVA_SAM [15], RCVA [16], DCVA [1], and TLCVA [17].

images is different, the quantitative detection accuracies are varied with the size of inputting images. That is because the size of inputting images is different, and so the content of the image scene will be different. As the robustness of each approach is limited, when the content

of an image scene is varied, the detection accuracies will also be different.

- 3) The optimal input size for a specific method differs for distinct datasets and different measurements. When the size of the input images is 400×400 pixels, DCVA [1]

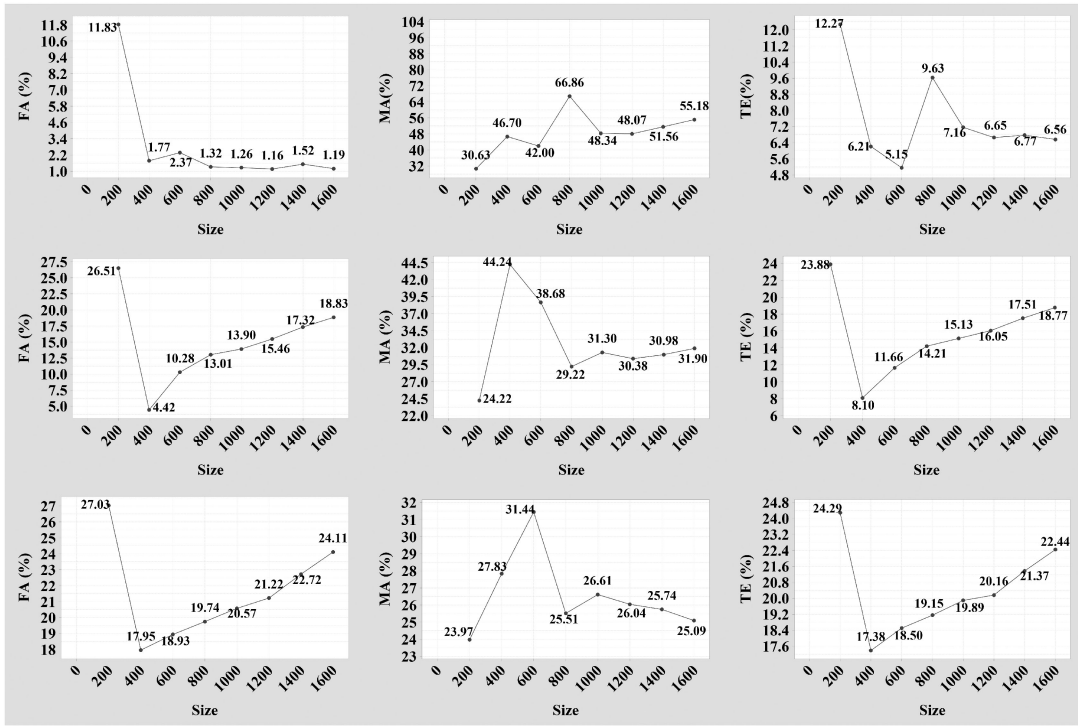


Fig. 6. Relationship between detection accuracies and image size for Landsat images with a 30-m/pixel resolution. The first, second, and third rows represent the diagnosis on DCVA [1], RCVA [16], and CVA_SAM [15], respectively.

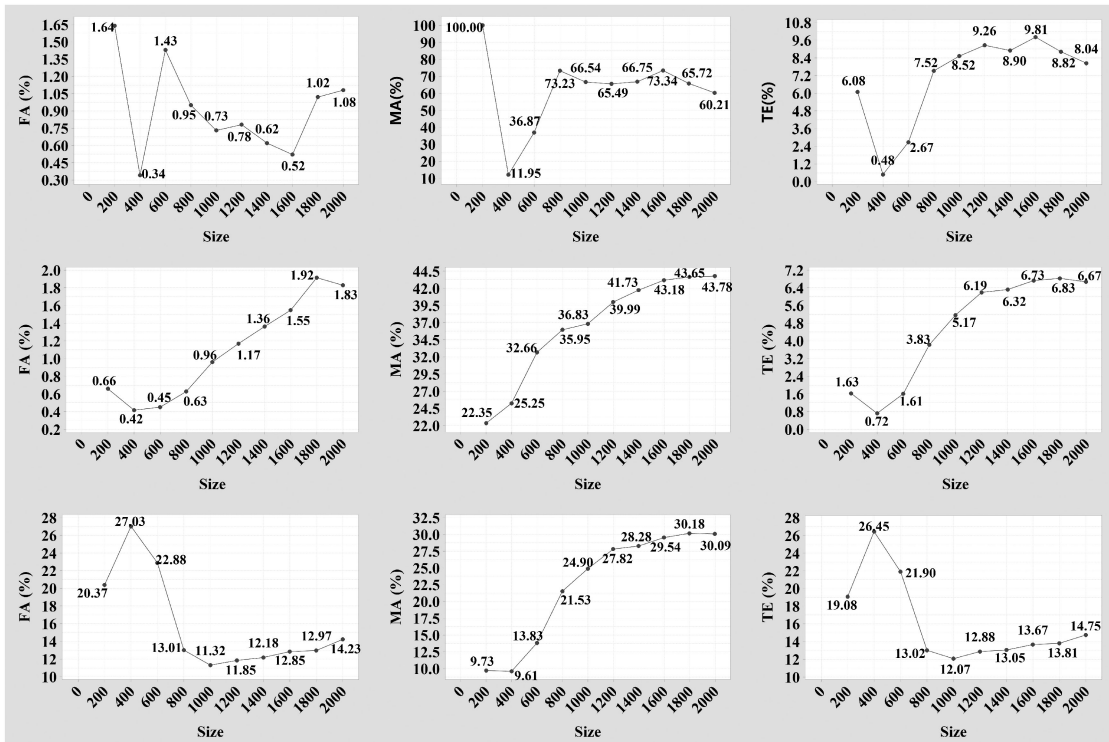


Fig. 7. Relationship between detection accuracies and image size for Spot-5 images with a 2.5-m/pixel resolution. The first, second, and third rows represent the diagnosis on DCVA [1], RCVA [16], and CVA_SAM [15], respectively.

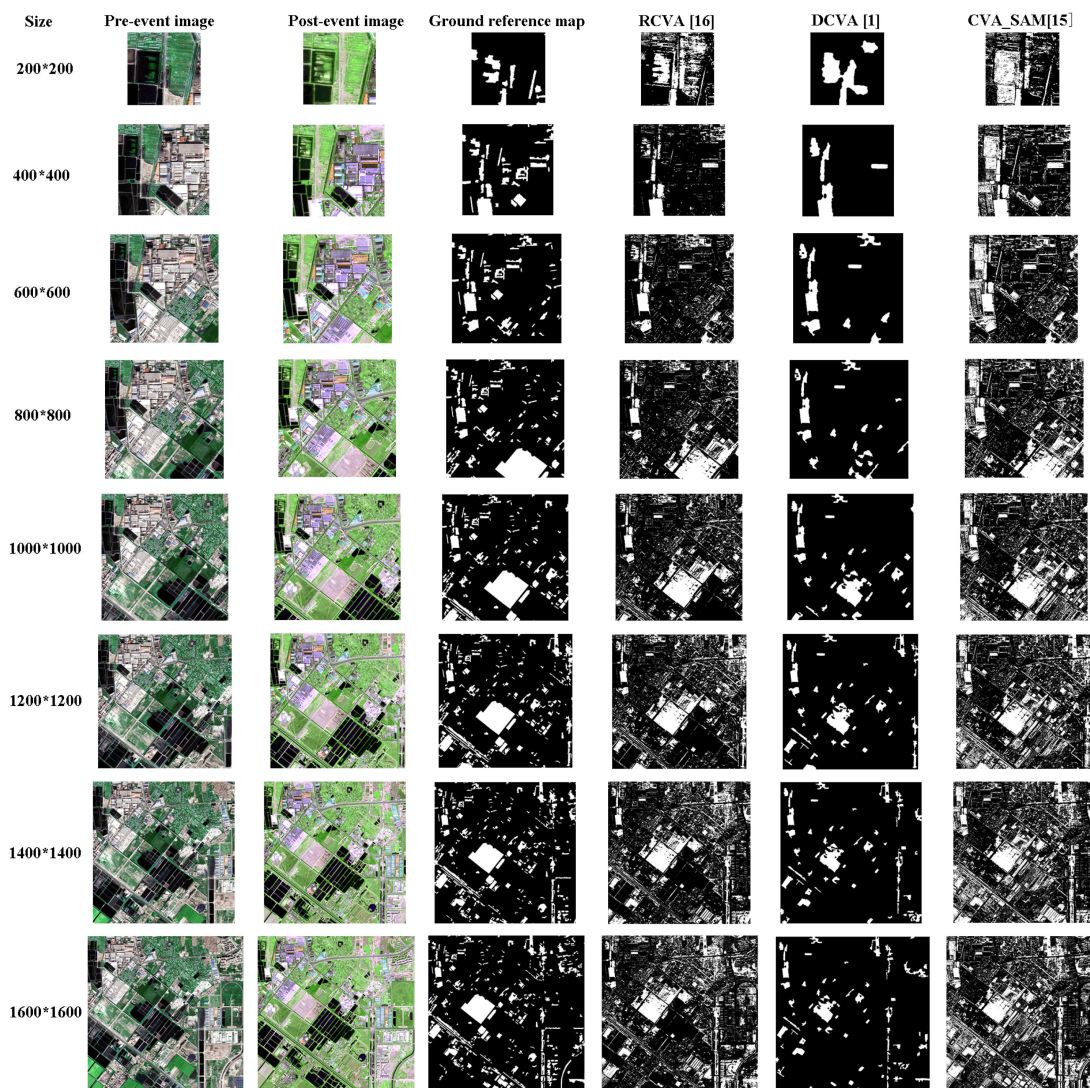


Fig. 8. Visual performance for applying RCVA [16], DCVA [1], and CVA_SAM [15] on the different sizes of Landsat images.

reaches its best performance in terms of FA, MA, and TE for the Landsat image in Fig. 6. However, CVA_SAM [15] acquires its best performance in terms of FA and TE when the size of the input images is 1000×1000 pixels, and its MA meet its best performance when the size of the input image is 200×200 pixels. The response of DCVA [1], RCVA [16], and CVA_SAM [15] to the Spot images further verifies this observation, as shown in Fig. 7.

The results of the diagnosis on the selected CVA-based LCCD methods by the two experiments indicate that the nature of the considered remote sensing image plays an important role in the progress of detecting land cover change while disregarding the special characteristic of a specific method. Furthermore, different methods have distinct optimal sizes of input images to acquire the best detection performance. This finding may be helpful for determining the size of input images when applying a method to an image scene.

V. CONCLUSION

In this article, we briefly reviewed the CVA-based LCCD methods with remote sensing images, and then, some of the widely used techniques, including the classical CVA [13], CVA_MRF [14], CVA_SAM [15], RCVA [16], DCVA [1], and TLCVA [17], were diagnosed with remote sensing images of different resolutions. The main contribution of this article lies in two aspects: First, it reviewed the CVA methods and the CVA-based LCCD methods briefly, and provides an overview of the CVA-based LCCD methods, this systematic induction of the development of CVA may be helpful for peer researcher, especially for the preliminary researcher. Second, we presented a comprehensive discussion on the relationship between detection accuracies and the size of input images. As far as we know, this study is the first investigation on the relationship between the input image size and detection accuracies for LCCD with remote sensing images. This article may provide a general guidance in

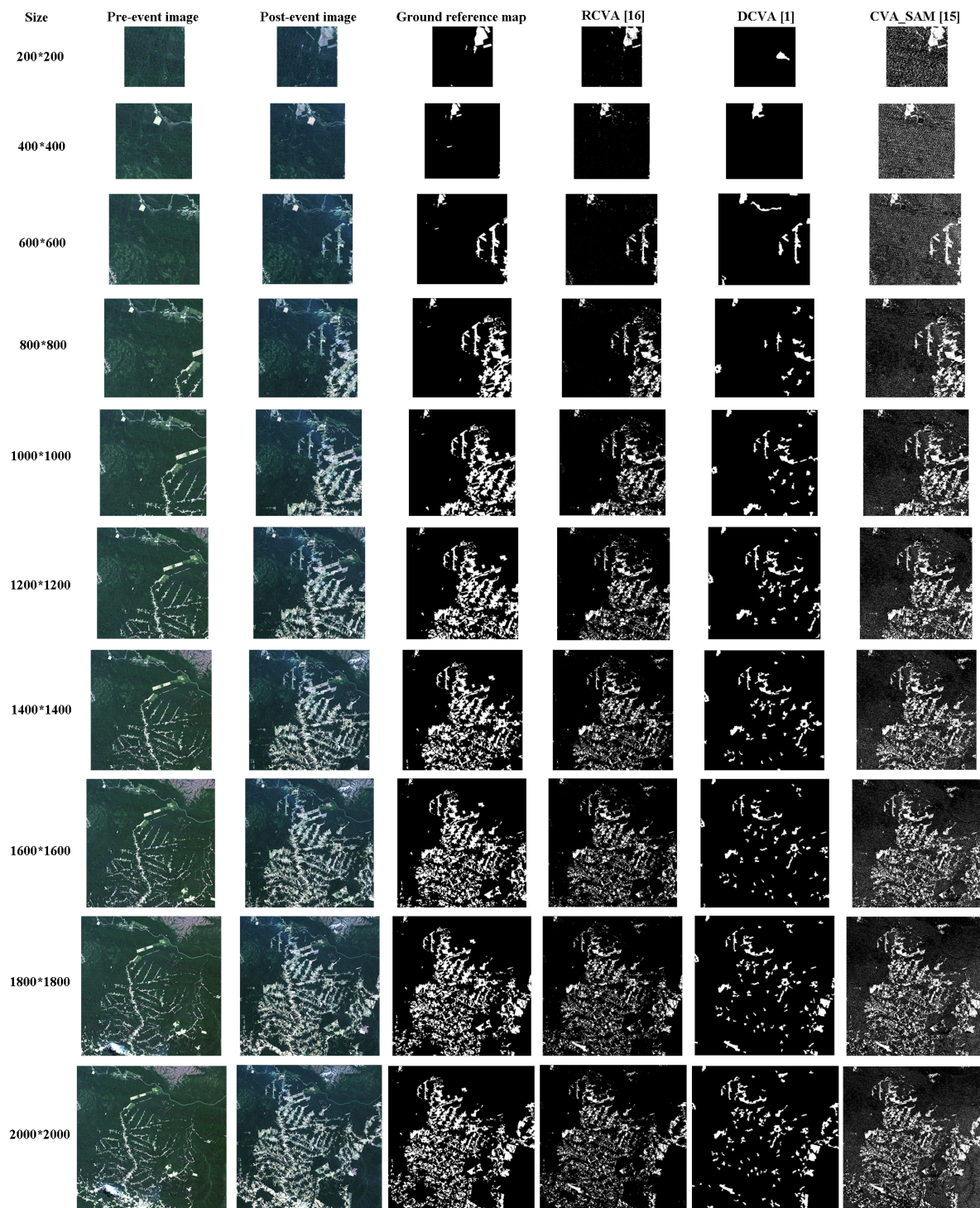


Fig. 9. Visual performance for applying RCVA [16], DCVA [1], and CVA_SAM [15] on the different sizes of Spot-5 images.

acquiring the best detection performance for practitioners who apply CVA-based LCCD methods to a large area.

In addition, based on the analysis of the experiments with six datasets, it can be concluded that there is no one CVA-based method that can be labeled as “good” or “bad,” and the performance of a method will be different when applying it on different datasets. Thus, selecting a suitable CVA-based method referred to the dataset, and the parameters’ setting for a specific dataset should acquire by trial-and-error experiments.

Although we reviewed the CVA techniques systemically, and several widely used CVA-based techniques for LCCD were selected for analysis and discussion, additional diagnoses should be further required for more comprehensive analysis when the referred datasets are available. For example, if several pairs of bitemporal images with different resolutions referring to the same change scenes are available, then additional details of detection results can be diagnosed, such as the noise spatial distribution and its relationship with spatial resolution. In our

future study, we will pay close attention to dataset collection and explore additional comprehensive characteristics of many CVA-based methods.

REFERENCES

- [1] S. Saha, F. Bovolo, and L. Bruzzone, "Unsupervised deep change vector analysis for multiple-change detection in VHR images," *IEEE Trans. Geosci. Remote Sens.*, vol. 57, no. 6, pp. 3677–3693, Jun. 2019.
- [2] J. Peng *et al.*, "Low-rank and sparse representation for hyperspectral image processing: A review," *IEEE Geosci. Remote Sens. Mag.*, to be published, doi: [10.1109/MGRS.2021.3075491](https://doi.org/10.1109/MGRS.2021.3075491).
- [3] J. Peng, Y. Zhou, W. Sun, Q. Du, and L. Xia, "Self-paced nonnegative matrix factorization for hyperspectral unmixing," *IEEE Trans. Geosci. Remote Sens.*, vol. 59, no. 2, pp. 1501–1515, Feb. 2021.
- [4] L. ZhiYong, T. Liu, J. A. Benediktsson, and N. Falco, "Land cover change detection techniques: Very-high-resolution optical images: A review," *IEEE Geosci. Remote Sens. Mag.*, to be published, doi: [10.1109/MGRS.2021.3088865](https://doi.org/10.1109/MGRS.2021.3088865).
- [5] Z. Zhu, "Change detection using landsat time series: A review of frequencies, preprocessing, algorithms, and applications," *ISPRS J. Photogramm. Remote Sens.*, vol. 130, no. 8, pp. 370–384, 2017.
- [6] L. Zhiyong, T. Liu, R. Y. Wang, J. A. Benediktsson, and S. Saha, "Automatic landslide inventory mapping approach based on change detection technique with very-high-resolution images," *IEEE Geosci. Remote Sens. Lett.*, to be published, doi: [10.1109/LGRS.2020.3041409](https://doi.org/10.1109/LGRS.2020.3041409).
- [7] L. Cai, W. Shi, H. Zhang, and M. Hao, "Object-oriented change detection method based on adaptive multi-method combination for remote-sensing images," *Int. J. Remote Sens.*, vol. 37, no. 22, pp. 5457–5471, 2016.
- [8] P. Canuti, N. Casagli, L. Ermini, R. Fanti, and P. Farina, "Landslide activity as a geoinicator in Italy: Significance and new perspectives from remote sensing," *Environ. Geol.*, vol. 45, no. 7, pp. 907–919, 2004.
- [9] B. Chen, Z. Chen, L. Deng, Y. Duan, and J. Zhou, "Building change detection with RGB-d map generated from UAV images," *Neurocomputing*, vol. 208, pp. 350–364, 2016.
- [10] L. Dong and J. Shan, "A comprehensive review of earthquake-induced building damage detection with remote sensing techniques," *ISPRS J. Photogramm. Remote Sens.*, vol. 84, pp. 85–99, 2013.
- [11] N. Falco, M. Dalla Mura, F. Bovolo, J. A. Benediktsson, and L. Bruzzone, "Change detection in VHR images based on morphological attribute profiles," *IEEE Geosci. Remote Sens. Lett.*, vol. 10, no. 3, pp. 636–640, May 2013.
- [12] X.-L. Chen, H.-M. Zhao, P.-X. Li, and Z.-Y. Yin, "Remote sensing image-based analysis of the relationship between urban heat island and land use/cover changes," *Remote Sens. Environ.*, vol. 104, no. 2, pp. 133–146, 2006.
- [13] W. A. Malila, "Change vector analysis: An approach for detecting forest changes with landsat," in *Proc. LARS Symp.*, 1980, pp. 385–397.
- [14] L. Bruzzone and D. F. Prieto, "Automatic analysis of the difference image for unsupervised change detection," *IEEE Trans. Geosci. Remote Sens.*, vol. 38, no. 3, pp. 1171–1182, May 2000.
- [15] H. Zhuang, K. Deng, H. Fan, and M. Yu, "Strategies combining spectral angle mapper and change vector analysis to unsupervised change detection in multispectral images," *IEEE Geosci. Remote Sens. Lett.*, vol. 13, no. 5, pp. 681–685, May 2016.
- [16] F. Thonfeld, H. Feilhauer, M. Braun, and G. Menz, "Robust change vector analysis (RCVA) for multi-sensor very high resolution optical satellite data," *Int. J. Appl. Earth Observ. Geoinf.*, vol. 50, pp. 131–140, 2016.
- [17] P. Du, X. Wang, D. Chen, S. Liu, C. Lin, and Y. Meng, "An improved change detection approach using tri-temporal logic-verified change vector analysis," *ISPRS J. Photogramm. Remote Sens.*, vol. 161, pp. 278–293, 2020.
- [18] E. F. Lambin and A. H. Strahlers, "Change-vector analysis in multitemporal space: A tool to detect and categorize land-cover change processes using high temporal-resolution satellite data," *Remote Sens. Environ.*, vol. 48, no. 2, pp. 231–244, 1994.
- [19] E. F. Lambin and A. H. Strahler, "Indicators of land-cover change for change-vector analysis in multitemporal space at coarse spatial scales," *Int. J. Remote Sens.*, vol. 15, no. 10, pp. 2099–2119, 1994.
- [20] Y. Bayarjargal, A. Karnieli, M. Bayasgalan, S. Khudulmur, C. Gandush, and C. Tucker, "A comparative study of NOAA-AVHRR derived drought indices using change vector analysis," *Remote Sens. Environ.*, vol. 105, no. 1, pp. 9–22, 2006.
- [21] T. R. Allen and J. A. Kupfer, "Application of spherical statistics to change vector analysis of landsat data: Southern Appalachian Spruce-Fir Forests," *Remote Sens. Environ.*, vol. 74, no. 3, pp. 482–493, 2000.
- [22] R. D. Johnson and E. Kasischke, "Change vector analysis: A technique for the multispectral monitoring of land cover and condition," *Int. J. Remote Sens.*, vol. 19, no. 3, pp. 411–426, 1998.
- [23] P. C. Smits and A. Annoni, "Toward specification-driven change detection," *IEEE Trans. Geosci. Remote Sens.*, vol. 38, no. 3, pp. 1484–1488, May 2000.
- [24] Y. Zhao and C. He, "Improving change vector analysis in multi-temporal space to detect land cover changes by using cross-correlogram spectral matching algorithm," in *Proc. IEEE Int. Geosci. Remote Sens. Symp.*, 2011, pp. 174–177.
- [25] Z. Wu, Z. Hu, and Q. Fan, "Superpixel-based unsupervised change detection using multi-dimensional change vector analysis and SVM-based classification," *ISPRS Ann. Photogramm. Remote Sens. Spatial Inf. Sci.*, vol. 7, pp. 257–262, 2012.
- [26] S. Liu, L. Bruzzone, F. Bovolo, and P. Du, "A novel sequential spectral change vector analysis for representing and detecting multiple changes in hyperspectral images," in *Proc. IEEE Geosci. Remote Sens. Symp.*, 2014, pp. 4656–4659.
- [27] S. Liu, L. Bruzzone, F. Bovolo, M. Zanetti, and P. Du, "Sequential spectral change vector analysis for iteratively discovering and detecting multiple changes in hyperspectral images," *IEEE Trans. Geosci. Remote Sens.*, vol. 53, no. 8, pp. 4363–4378, Aug. 2015.
- [28] O. A. Carvalho Júnior, R. F. Guimarães, A. R. Gillespie, N. C. Silva, and R. A. Gomes, "A new approach to change vector analysis using distance and similarity measures," *Remote Sens.*, vol. 3, no. 11, pp. 2473–2493, 2011.
- [29] K. Sun and Y. Chen, "The application of objects change vector analysis in object-level change detection," in *Proc. Int. Conf. Comput. Intell. Ind. Appl.*, 2010, pp. 6–7.
- [30] L. Li, X. Li, Y. Zhang, L. Wang, and G. Ying, "Change detection for high-resolution remote sensing imagery using object-oriented change vector analysis method," in *Proc. IEEE Int. Geosci. Remote Sens. Symp.*, 2016, pp. 2873–2876.
- [31] H. Sun, W. Zhou, Y. Zhang, C. Cai, and Q. Chen, "Integrating spectral and textural attributes to measure magnitude in object-based change vector analysis," *Int. J. Remote Sens.*, vol. 40, no. 15, pp. 5749–5767, 2019.
- [32] D. C. Zanotta, L. Bruzzone, and F. Bovolo, "Detection of specific changes in image time series by an adaptive change vector analysis," in *Proc. IEEE Int. Geosci. Remote Sens. Symp.*, 2014, pp. 1285–1288.
- [33] Q. Chen and Y. Chen, "Multi-feature object-based change detection using self-adaptive weight change vector analysis," *Remote Sens.*, vol. 8, no. 7, p. 549–568, 2016.
- [34] S. Liu, Q. Du, X. Tong, A. Samat, L. Bruzzone, and F. Bovolo, "Multiscale morphological compressed change vector analysis for unsupervised multiple change detection," *IEEE J. Sel. Topics Appl. Earth Observ. Remote Sens.*, vol. 10, no. 9, pp. 4124–4137, Sep. 2017.
- [35] K. Nackaerts, K. Vaesen, B. Muys, and P. Coppin, "Comparative performance of a modified change vector analysis in forest change detection," *Int. J. Remote Sens.*, vol. 26, no. 5, pp. 839–852, 2005.
- [36] A. Akkartal and F. Sunar, "Land cover change assessment in Belek forest based on change vector analysis," in *Remote Sensing for a Changing Europe*. Amsterdam, The Netherlands: IOS Press, 2009, pp. 571–577.
- [37] D. Marinelli, N. C. Coops, D. K. Bolton, and L. Bruzzone, "An unsupervised change detection method for Lidar data in forest areas based on change vector analysis in the polar domain," in *Proc. IEEE Int. Geosci. Remote Sens. Symp.*, 2018, pp. 1922–1925.
- [38] M. Zanetti, L. Bruzzone, and D. Fernández-Prieto, "A multivariate change vector analysis system for unsupervised detection of clear-cuts in Sentinel-2," in *Proc. IEEE Int. Geosci. Remote Sens. Symp.*, 2018, pp. 1942–1945.
- [39] P. Perbet, M. Fortin, A. Ville, and M. Béland, "Near real-time deforestation detection in Malaysia and Indonesia using change vector analysis with three sensors," *Int. J. Remote Sens.*, vol. 40, no. 19, pp. 7439–7458, 2019.
- [40] C. Yun-Hao, L. Xiao-Bing, and X. Feng, "NDVI changes in China between 1989 and 1999 using change vector analysis based on time series data," *J. Geographical Sci.*, vol. 11, no. 4, pp. 383–392, 2001.
- [41] H. Yu and Y. Jia, "Vegetation change detection for urban areas based on extended change vector analysis," *Geoinform., Remotely Sensed Data Inf.*, vol. 6419, 2006, Art. no. 64190E.
- [42] Y. Zhao, C. He, and Q. Zhang, "Monitoring vegetation dynamics by coupling linear trend analysis with change vector analysis: A case study in the Xilingol steppe in northern China," *Int. J. Remote Sens.*, vol. 33, no. 1, pp. 287–308, 2012.
- [43] X. Gu, W. Li, and L. Wang, "Understanding vegetation changes in Northern China and Mongolia with change vector analysis," *SpringerPlus*, vol. 5, no. 1, pp. 1–13, 2016.

- [44] X. Yang, A. M. Smith, and M. J. Hill, "Updating the grassland vegetation inventory using change vector analysis and functionally-based vegetation indices," *Can. J. Remote Sens.*, vol. 43, no. 1, pp. 62–78, 2017.
- [45] S. Rahman and V. Mesev, "Change vector analysis, tasseled cap, and NDVI-NDMI for measuring land use/cover changes caused by a sudden short-term severe drought: 2011 Texas event," *Remote Sens.*, vol. 11, no. 19, 2019, Art. no. 2217.
- [46] X. Gu, Y. Pan, L. Han, and C. Xu, "Study on growth monitoring of winter wheat based on change vector analysis," *Geospatial Inf. Technol. Appl.*, vol. 6754, 2007, Art. no. 67540X.
- [47] C. Baker, R. L. Lawrence, C. Montagne, and D. Patten, "Change detection of wetland ecosystems using Landsat imagery and change vector analysis," *Wetlands*, vol. 27, no. 3, pp. 610–619, 2007.
- [48] S. E. Flores and S. R. Yool, "Sensitivity of change vector analysis to land cover change in an arid ecosystem," *Int. J. Remote Sens.*, vol. 28, no. 5, pp. 1069–1088, 2007.
- [49] H. Xu, Y. Wang, H. Guan, T. Shi, and X. Hu, "Detecting ecological changes with a remote sensing based ecological index (RSEI) produced time series and change vector analysis," *Remote Sens.*, vol. 11, no. 20, 2019, Art. no. 2345.
- [50] T. Landmann, M. Schramm, C. Huettich, and S. Dech, "MODIS-based change vector analysis for assessing wetland dynamics in Southern Africa," *Remote Sens. Lett.*, vol. 4, no. 2, pp. 104–113, 2013.
- [51] I. Vorovencii, "Applying the change vector analysis technique to assess the desertification risk in the south-west of Romania in the period 1984–2011," *Environ. Monit. Assessment*, vol. 189, no. 10, pp. 1–18, 2017.
- [52] M. Taberner and F. Sunar, "An implementation of the change vector analysis technique to assess the changes in land cover with multitemporal remotely sensed images, a case study- Istanbul, Turkey," *Inf. Sustain.*, vol. 3, no. 7, pp. 605–614, 1998.
- [53] X. Zhan *et al.*, "Land cover change detection with change vector in the red and near-infrared reflectance space," in *Proc. IEEE Int. Geosci. Remote Sens. Symp.*, 1998, vol. 2, pp. 859–861.
- [54] I. Vorovencii, "A change vector analysis technique for monitoring land cover changes in Copsa Mica, Romania, in the period 1985–2011," *Environ. Monit. Assessment*, vol. 186, no. 9, pp. 5951–5968, 2014.
- [55] G.-W. Yoon, Y. B. Yun, and J.-H. Park, "Change vector analysis: Detecting of areas associated with flood using landsat TM," in *Proc. IEEE Int. Geosci. Remote Sens. Symp.*, 2003, vol. 5, pp. 3386–3388.
- [56] C. Huang, X. Zan, X. Yang, and S. Zhang, "Surface water change detection using change vector analysis," in *Proc. IEEE Int. Geosci. Remote Sens. Symp.*, 2016, pp. 2834–2837.
- [57] C. He, A. Wei, P. Shi, Q. Zhang, and Y. Zhao, "Detecting land-use/land-cover change in rural-urban fringe areas using extended change-vector analysis," *Int. J. Appl. Earth Observ. Geoinf.*, vol. 13, no. 4, pp. 572–585, 2011.
- [58] E. E. Maeda, G. F. Arcoverde, P. K. Pellikka, and Y. E. Shimabukuro, "Fire risk assessment in the Brazilian Amazon using MODIS imagery and change vector analysis," *Appl. Geogr.*, vol. 31, no. 1, pp. 76–84, 2011.
- [59] Q. Chen and Y. Chen, "A Multi-feature optimization approach to object-based image classification," *Int. Conf. Image and Video Retrieval*, 2006, pp. 310–319.
- [60] S. Ertürk, "Fuzzy fusion of change vector analysis and spectral angle mapper for hyperspectral change detection," in *Proc. IEEE Int. Geosci. Remote Sens. Symp.*, 2018, pp. 5045–5048.
- [61] F. Zakeri, B. Huang, and M. R. Saradjian, "Fusion of change vector analysis in posterior probability space and postclassification comparison for change detection from multispectral remote sensing data," *Remote Sens.*, vol. 11, no. 13, pp. 1511–1525, 2019.
- [62] S. Saha, F. Bovolo, and L. Bruzzone, "Building change detection in VHR SAR images via unsupervised deep transcoding," *IEEE Trans. Geosci. Remote Sens.*, vol. 59, no. 3, pp. 1917–1929, Mar. 2021.
- [63] Z. Qi, A. G. O. X. Yeh, X. Li, and X. Zhang, "A three-component method for timely detection of land cover changes using polarimetric SAR images," *ISPRS J. Photogramm. Remote Sens.*, vol. 107, pp. 3–21, 2015.
- [64] D. Marinelli, C. Paris, and L. Bruzzone, "A novel approach to 3-D change detection in multitemporal Lidar data acquired in forest areas," *IEEE Trans. Geosci. Remote Sens.*, vol. 56, no. 6, pp. 3030–3046, Jun. 2018.
- [65] G. A. Parra, M. Mouchot, and C. Roux, "A multitemporal land-cover change analysis tool using change vector and principal components analysis," in *Proc. IEEE Int. Geosci. Remote Sens. Symp.*, 1996, vol. 3, pp. 1753–1755.
- [66] J. Chen, P. Gong, C. He, R. Pu, and P. Shi, "Land-use/land-cover change detection using improved change-vector analysis," *Photogramm. Eng. Remote Sens.*, vol. 69, no. 4, pp. 369–379, 2003.
- [67] C. He, Y. Zhao, J. Tian, P. Shi, and Q. Huang, "Improving change vector analysis by cross-correlogram spectral matching for accurate detection of land-cover conversion," *Int. J. Remote Sens.*, vol. 34, no. 4, pp. 1127–1145, 2013.
- [68] R. Xu, H. Lin, Y. Lü, Y. Luo, Y. Ren, and A. Comber, "A modified change vector approach for quantifying land cover change," *Remote Sens.*, vol. 10, no. 10, pp. 1578–1598, 2018.
- [69] T. Warner, "Hyperspherical direction cosine change vector analysis," *Int. J. Remote Sens.*, vol. 26, no. 6, pp. 1201–1215, 2005.
- [70] A. Varshney, M. K. Arora, and J. K. Ghosh, "Median change vector analysis algorithm for land-use land-cover change detection from remote-sensing data," *Remote Sens. Lett.*, vol. 3, no. 7, pp. 605–614, 2012.
- [71] F. Bovolo and L. Bruzzone, "A theoretical framework for unsupervised change detection based on change vector analysis in the polar domain," *IEEE Trans. Geosci. Remote Sens.*, vol. 45, no. 1, pp. 218–236, Jan. 2006.
- [72] L. Jing and Q. Cheng, "Image fusion based on pixel spectra change vector and multivariate regression of panchromatic and visible-near IR multispectral bands," in *Proc. IEEE Int. Geosci. Remote Sens. Symp.*, 2006, pp. 2923–2926.
- [73] R. N. Siwe and B. Koch, "Change vector analysis to categorise land cover change processes using the tasseled cap as biophysical indicator," *Environ. Monit. Assessment*, vol. 145, no. 1, pp. 227–235, 2008.
- [74] C. Kontoes, "Operational land cover change detection using change vector analysis," *Int. J. Remote Sens.*, vol. 29, no. 16, pp. 4757–4779, 2008.
- [75] S. Ye, D. Chen, and J. Yu, "A targeted change-detection procedure by combining change vector analysis and post-classification approach," *ISPRS J. Photogramm. Remote Sens.*, vol. 114, pp. 115–124, 2016.
- [76] J. Chen, X. Chen, X. Cui, and J. Chen, "Change vector analysis in posterior probability space: A new method for land cover change detection," *IEEE Geosci. Remote Sens. Lett.*, vol. 8, no. 2, pp. 317–321, Mar. 2011.
- [77] S. Azzouzi, A. Vidal, and H. Bentounes, "A modified approach for change detection using change vector analysis in posterior probability space," *Int. Arch. Photogramm. Remote Sens. Spatial Inf. Sci.*, vol. XL-7/W3, pp. 593–598, 2015.
- [78] L. Castellana, A. D'Addabbo, and G. Pasquariello, "A composed supervised/unsupervised approach to improve change detection from remote sensing," *Pattern Recognit. Lett.*, vol. 28, no. 4, pp. 405–413, 2007.
- [79] V.-E. Neagoe, A.-D. Ciotec, and S.-V. Carata, "A new multispectral pixel change detection approach using pulse-coupled neural networks for change vector analysis," in *Proc. IEEE Int. Geosci. Remote Sens. Symp.*, 2016, pp. 3386–3389.
- [80] L. Su, J. Shi, P. Zhang, Z. Wang, and M. Gong, "Detecting multiple changes from multi-temporal images by using stacked denoising autoencoder based change vector analysis," in *Proc. Int. Joint Conf. Neural Netw.*, 2016, pp. 1269–1276.
- [81] A. C. Siravenha and E. G. Pelaes, "Analysing environmental changes in the neighbourhood of mines using compressed change vector analysis: Case study of Carajas mountains, Brazil," *Int. J. Remote Sens.*, vol. 39, no. 12, pp. 4170–4193, 2018.
- [82] S. Singh and R. Talwar, "An intercomparison of different topography effects on discrimination performance of fuzzy change vector analysis algorithm," *Meteorol. Atmos. Phys.*, vol. 130, no. 1, pp. 125–136, 2018.
- [83] D. Lu, P. Mausel, E. Brondizio, and E. Moran, "Change detection techniques," *Int. J. Remote Sens.*, vol. 25, no. 12, pp. 2365–2401, 2004.
- [84] P. Coppin, I. Jonckheere, K. Nackaerts, B. Muys, and E. Lambin, "Review article: digital change detection methods in ecosystem monitoring: A review," *Int. J. Remote Sens.*, vol. 25, no. 9, pp. 1565–1596, 2004.
- [85] M. C. Hansen and T. R. Loveland, "A review of large area monitoring of land cover change using landsat data," *Remote Sens. Environ.*, vol. 122, pp. 66–74, 2012.
- [86] A. P. Tewkesbury, A. J. Comber, N. J. Tate, A. Lamb, and P. F. Fisher, "A critical synthesis of remotely sensed optical image change detection techniques," *Remote Sens. Environ.*, vol. 160, pp. 1–14, 2015.
- [87] N. Otsu, "A threshold selection method from gray-level histograms," *IEEE Trans. Syst., Man, Cybern.*, vol. 9, no. 1, pp. 62–66, Jan. 1979.
- [88] M. Volpi, D. Tuia, G. Camps-Valls, and M. Kanevski, "Unsupervised change detection with kernels," *IEEE Geosci. Remote Sens. Lett.*, vol. 9, no. 6, pp. 1026–1030, Nov. 2012.
- [89] G. Xian, C. Homer, and J. Fry, "Updating the 2001 national land cover database land cover classification to 2006 by using landsat imagery change detection methods," *Remote Sens. Environ.*, vol. 113, no. 6, pp. 1133–1147, 2009.
- [90] Y. Bazi, F. Melgani, and H. D. Al-Sharari, "Unsupervised change detection in multispectral remotely sensed imagery with level set methods," *IEEE Trans. Geosci. Remote Sens.*, vol. 48, no. 8, pp. 3178–3187, Aug. 2010.



Lv ZhiYong (Member, IEEE) received the M.S. and Ph.D. degrees from the School of Remote sensing and Information Engineering, Wuhan University, Wuhan, China, in 2008 and 2014, respectively.

He is an Engineer of surveying and worked with The First Institute of Photogrammetry and Remote Sensing from 2008 to 2011. He is currently working with the School of Computer Science and Engineering, Xi'an University of Technology, Xi'an, China. His research interests include multihyperspectral and high-resolution remotely sensed image processing,

spatial feature extraction, neural networks, pattern recognition, deep learning, and remote sensing applications.



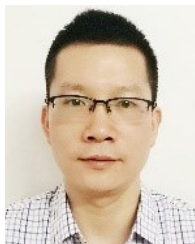
Fengjun Wang is currently working toward the master's degree in computer science with the Xi'an University of Technology, Xi'an, China.

His research interests include spatial-spectral feature extraction, pattern recognition, ground target detection, and land cover/land use change detection, through remote sensing image with high or very high spatial resolution (including satellite imagery and aerial images).



LinFu Xie received the bachelor's and Ph.D. degrees from Wuhan University, Wuhan, China, in 2013 and 2019, respectively.

He joined the School of Architecture and Urban Planning, Shenzhen University, Shenzhen, China, as a Postdoctor in 2019. His research interests include image processing, multiplatform photogrammetry, and 3-D city modeling.



WeiWei Sun (Senior Member, IEEE) received the B.S. degree in surveying and mapping from and the Ph.D. degree in cartography and geographic information engineering from Tongji University, Shanghai, China, in 2007 and 2013, respectively.

From 2011 to 2012, he was with the Department of Applied Mathematics, University of Maryland, College Park, working as a Visiting Scholar with the famous Prof. J. Benedetto to study on the dimensionality reduction of hyperspectral image. From 2014 to 2016, he was with the State Key Laboratory for Information Engineering in Surveying, Mapping and Remote Sensing (LIESMARS), Wuhan University, working as a Postdoctor to study intelligent processing in hyperspectral imagery. From 2017 to 2018, he worked as a Visiting Scholar with the Department of Electrical and Computer Engineering, Mississippi State University. He is currently a Full Professor with Ningbo University, Ningbo, China. He has authored and co-authored more than 70 journal papers. His current research interests include hyperspectral image processing with manifold learning, anomaly detection, and target recognition of remote sensing imagery using compressive sensing.

From 2011 to 2012, he was with the Department of Applied Mathematics, University of Maryland, College Park, working as a Visiting Scholar with the famous Prof. J. Benedetto to study on the dimensionality reduction of hyperspectral image. From 2014 to 2016, he was with the State Key Laboratory for Information Engineering in Surveying, Mapping and Remote Sensing (LIESMARS), Wuhan University, working as a Postdoctor to study intelligent processing in hyperspectral imagery. From 2017 to 2018, he worked as a Visiting Scholar with the Department of Electrical and Computer Engineering, Mississippi State University. He is currently a Full Professor with Ningbo University, Ningbo, China. He has authored and co-authored more than 70 journal papers. His current research interests include hyperspectral image processing with manifold learning, anomaly detection, and target recognition of remote sensing imagery using compressive sensing.



Nicola Falco (Member, IEEE) received the B.Sc. and M.Sc. degrees in telecommunication engineering from the University of Trento, Italy, in 2008 and 2011, respectively, and the joint Ph.D. degree in electrical and computer engineering from the University of Iceland, Reykjavik, Iceland, and in information and communication technologies from the University of Trento, in 2015.

He is currently a Research Scientist with Lawrence Berkeley National Laboratory in the Climate & Ecosystem Sciences Division, Berkeley, California.

His research focuses on the development of methodologies based on image/signal processing, pattern recognition, and machine learning for multi-source data analysis and integration, including remote sensing (hyperspectral,

LiDAR, high-res) and geophysical data, with applications in environmental monitoring, climate change, and precision agriculture.

Dr. Falco was the recipient of the Recognition of IEEE GEOSCIENCE REMOTE SENSING LETTERS Best Reviewers in 2013, and co-recipient of the Third Prize in the Student Paper Competition of the 2015 IEEE International Geoscience and Remote Sensing Symposium. He is a referee for several international journals, including IEEE TRANSACTION ON GEOSCIENCE AND REMOTE SENSING, IEEE GEOSCIENCE AND REMOTE SENSING LETTERS, IEEE JOURNAL OF SELECTED TOPIC IN APPLIED EARTH OBSERVATIONS AND REMOTE SENSING, *International Journal of Applied Earth Observation and Geoinformation* (Elsevier), *Pattern Recognition Letters* (Elsevier), *International Journal of Remote Sensing and Remote Sensing Letters* (Taylor & Francis), *Agriculture (MDPI)*, *Remote Sensing (MDPI)*, *Scientific Reports (Nature)*.



Jón Atli Benediktsson (Fellow, IEEE) received the Cand.Sci. degree in electrical engineering from the University of Iceland, Reykjavik, Iceland, in 1984, and the M.S.E.E. and Ph.D. degrees from Purdue University, West Lafayette, IN, USA, in 1987 and 1990, respectively.

He is currently a Pro Rector for Academic Affairs and a Professor of electrical and computer engineering with the University of Iceland. He is a founder of the biomedical startup company Oxymap (www.oxymap.com). His research interests include

remote sensing, biomedical analysis of signals, pattern recognition, image processing, and signal processing, and he has authored and co-authored extensively in these fields.

Prof. Benediktsson was the President of the IEEE Geoscience and Remote Sensing Society (GRSS) in 2011–2012, and has been on the GRSS AdCom since 2000. He was Editor for the IEEE TRANSACTIONS ON GEOSCIENCE AND REMOTE SENSING (TGRS) from 2003 to 2008 and has been serving as an Associate Editor for TGRS since 1999, the *IEEE Geoscience and Remote Sensing Letters* since 2003, and *IEEE Access* since 2013. He is on the International Editorial Board for the *International Journal of Image and Data Fusion* and was the Chairman of the Steering Committee for the *IEEE Journal of Selected Topics in Applied Earth Observations and Remote Sensing* in 2007–2010. He is a Fellow of the Society of Photo-optical Instrumentation Engineers and a Member of the Association of Chartered Engineers in Iceland (VFI), Societas Scintiarum Islandica, and Tau Beta Pi. He was the recipient of the Stevan J. Kristof Award from Purdue University in 1991 as an Outstanding Graduate Student in remote sensing; the Icelandic Research Council's Outstanding Young Researcher Award in 1997; the IEEE Third Millennium Medal in 2000; the yearly research award from the Engineering Research Institute of the University of Iceland in 2006; the Outstanding Service Award from the IEEE Geoscience and Remote Sensing Society in 2007; and IEEE/VFI Electrical Engineer of the Year Award in 2013. He was also the co-recipient of the the University of Iceland's Technology Innovation Award in 2004; the IEEE TRANSACTIONS ON GEOSCIENCE AND REMOTE SENSING Paper Award in 2012; and the IEEE GRSS Highest Impact Paper Award in 2013. He is a member of the Association of Chartered Engineers in Iceland (VFI), Societas Scintiarum Islandica and Tau Beta Pi.



ZhenZhen You received the B.S. degree in telecommunication from Xidian University, Xi'an, China, in 2011, the M.Eng. (Diplôme d'Ingénieur) and M.Res. degrees in image processing from IMT Atlantique (ex Tlcom Bretagne), Brest, France, in 2014, and the Ph.D. degree in computer science from Pierre and Marie Curie University (University of Paris VI), Paris, France, in 2017.

From 2014 to 2017, she did research with the Molecular Imaging Research Center (MIRcen), The French Alternative Energies and Atomic Energy

Commission, France. Since 2018, she has been a Lecturer with the Department of Computer Science and Engineering, Xi'an University of Technology, Xi'an, China. Her research interests include biomedical image processing, image segmentation, image enhancement, and machine learning.